Frequency-Domain Spectral Balance Using the Arithmetic Operator Method

CHAO-REN CHANG, MICHAEL B. STEER, MEMBER, IEEE, AND
GEORGE W. RHYNE, MEMBER, IEEE

Abstract — **A frequency-domain spectral balance method for the simulation of nonlinear analog circuits with multidimensional nonlinearities is presented. The method is coupled with a combination of Shamanskii and block Newton iteration schemes to produce an efficient general-purpose simulator. The technique is verified with measurements of a MESFET amplifier with single-tone and two-tone excitations.**

I. Introduction

MICROWAVE circuit designers have traditionally relied on the use of experimental modifications to ensure that their designs meet required specifications. This practice, however, is becoming increasingly impractical as circuit dimensions shrink and circuit complexity increases. Thus there is an increasing interest in the computer-aided design of microwave circuits. A frequency-domain spectral balance method is developed here for the evaluation of the current/voltage relation of multidimensional nonlinearities (e.g., current through a nonlinearity being a function of two or more voltages in the circuit). This is coupled with a combination of Shamanskii and modified Newton iteration schemes to yield an efficient and accurate simulator for the analysis of nonlinear circuits having multifrequency excitations.

Although the methods for analyzing nonlinear circuits are varied, they are all based on solving a set of nonlinear differential equations resulting from application of Kirchhoff's voltage law and Kirchhoff's current law using the constitutive relations (i.e., the element characteristics). The methods fall into three groups according to the way in which the nonlinear elements are treated: time-domain methods, hybrid (harmonic balance) methods, and frequency-domain methods. The work we report here is of the frequency-domain type; that is, it avoids explicit time-domain calculations. This is accomplished through expansion of the input–output characteristics of the nonlinear elements in a set of basis functions of which there are three basic types: Volterra series [1]–[6], algebraic functional expansion [7]–[9], and power series. With frequency-domain spectral balance analysis, power-series-based techniques are proving to be the most general methods for the analysis of nonlinear circuits with multifrequency large-signal excitations. This approach has been investigated by a number of researchers as the basis for hand calculations as well as for computer-based simulations [10]–[17]. We continued the development of this type of series [18], resulting in the form (called a generalized power series)[1]

$$Y_{\omega q} = \sum_{n=0}^{\infty} a_{\omega q, n} \left\{ \left[\sum_{k=0}^{K-1} x_k (t - \tau_k) \right]^n \right\}_{\omega q} \tag{1}$$

where $Y_{\omega q}$ is the frequency-domain system output at radian frequency ω_q, n is the order of each power series term, $a_{\omega q, n}$ is an ω_q and n dependent complex coefficient, τ_k is a time delay that depends on the input frequency ω_k, $x(t)$ is the independent variable, and the notation $\{f(x)\}_{\omega q}$ represents the phasor form of the ω_q component of the time-domain function $f(x)$. A complex power series with frequency-dependent time delays can simply incorporate many memory effects, and only a few terms of the series expansion may be required. Therefore, a much larger class of systems can be mathematically modeled by a generalized power series (GPS) expansion than by a conventional power series expansion. For most microwave applications, circuits are typically made up of only a few circuit elements so that simulation can proceed without using complex coefficients. Time delays can be included by phase shifting of the input signal.

With the GPS description of the nonlinear system, algebraic formulas for the system output when the input is a sum of sinusoids have been developed [18]–[20]. This method uses an input/output transform table (the intermodulation product descriptions) and is more accurately referred to as generalized power series analysis using the table method (GPSA-TM) to differentiate it from the extension developed here. The formulas used in GPSA-TM, however, are complicated and difficult to understand. In addition, using the transform table in this method produces many repetitive calculations which degrade the circuit analysis efficiency.

Manuscript received January 11, 1989; revised June 12, 1989. This work was supported by a National Science Foundation Presidential Young Investigator Award to M. B. Steer (Grant ECS-8657836) and by a grant from the Digital Equipment Corporation.

C.-R. Chang and M. B. Steer are with the Center for Communications and Signal Processing, Electrical and Computer Engineering Department, North Carolina State University, Raleigh, NC 27695-7911.

G. W. Rhyne was with the Electrical and Computer Engineering Department, North Carolina State University, Raleigh, NC. He is now with Texas Instruments, P.O. Box 655474, Dallas, TX 75266.

IEEE Log Number 8930526.

[1]The nomenclature has been changed slightly for compatibility with the work presented here.

0018-9480/89/1100-1681$01.00

GPSA-TM is practically restricted to one-dimensional (1-D) nonlinearities. It has been extended to two-dimensional (2-D) nonlinearities but the formulas are even more complicated [21] and its computer implementation is expected to be inefficient. In Section III, a newly developed frequency-domain spectral balance technique, the generalized power series analysis using the arithmetic operator method (GPSA-AOM) is presented. GPSA-AOM is straightforward, easy to implement, and handles multidimensional nonlinearities. It is also considerably faster than the GPSA-TM for single dimensional nonlinearities.

II. Development of Circuit Equations

One approach used to solve the system of nonlinear equations is to formulate the nonlinear problem so that a Newton iteration scheme can be used. In this section we develop a block matrix formulation of the nonlinear circuit equations and combine this with a Newton iteration scheme which uses a combination of full Newton iteration, block Newton iteration, and chord iteration [22] to obtain a fast nonlinear analog circuit simulator. In the formulation of the nonlinear circuit equations, no explicit separation of a circuit into linear and nonlinear subcircuits is made.

A. Circuit Equations

If K different frequency components exist in an analog nonlinear circuit, computer-aided analysis in the frequency domain solves a system of nonlinear equations:

$$\boldsymbol{M}(\boldsymbol{x})\boldsymbol{x} = \boldsymbol{y} \tag{2}$$

where

$$\boldsymbol{x} = \begin{bmatrix} \boldsymbol{x}_{\omega 0}^T & \boldsymbol{x}_{\omega 1}^T & \cdots & \boldsymbol{x}_{\omega(K-1)}^T \end{bmatrix}^T. \tag{3}$$

Here T indicates the transpose and $\boldsymbol{x}_{\omega k}$ is the variable vector to be solved which contains the necessary node voltages and edge currents at radian frequencies ω_k; the source vector $\boldsymbol{y}$, which includes all the independent sources, is similarly defined as $\boldsymbol{x}$ in (3); and the $\boldsymbol{x}$-dependent matrix $\boldsymbol{M}(\boldsymbol{x})$, the modified nodal admittance matrix [23], is the *circuit matrix* of the analog nonlinear network.

Solution of the nonlinear circuit equations (2) is based on the process of successive approximations. After each iteration i, a new approximation of the variable vector, ${}^i\boldsymbol{x}$, produces an *induced* source vector $\boldsymbol{y}({}^i\boldsymbol{x})$:

$$\boldsymbol{M}({}^i\boldsymbol{x}){}^i\boldsymbol{x} = \boldsymbol{y}({}^i\boldsymbol{x}). \tag{4}$$

Newton's method, or a variant of it, forms the basis of most iterative procedures in nonlinear circuit analysis. This method is based on the general relationship

$$\boldsymbol{f}(\boldsymbol{x}) = 0$$

where $\boldsymbol{f}({}^i\boldsymbol{x})$ is a vector with the same dimension as the variable vector $\boldsymbol{x}$. It is composed of the absolute values of the corresponding entries of the difference vector between the independent source vector $\boldsymbol{y}$ and the induced source vector $\boldsymbol{y}({}^i\boldsymbol{x})$. The iteration formula for Newton's method is

$${}^{i+1}\boldsymbol{x} = {}^i\boldsymbol{x} - \boldsymbol{J}^{-1}({}^i\boldsymbol{x})\,\boldsymbol{f}({}^i\boldsymbol{x}), \qquad i = 0,1,2,\cdots \tag{5}$$

where $\boldsymbol{J}({}^i\boldsymbol{x})$ is the Jacobian matrix of $\boldsymbol{f}$ in the ith iteration and $\boldsymbol{J}^{-1}({}^i\boldsymbol{x})$ is its inverse.

Fortunately, in solving the nonlinear circuit equations (2) using iterative procedures (5), the whole *circuit matrix* $\boldsymbol{M}({}^i\boldsymbol{x})$ need not be calculated. Both the Jacobian matrix $\boldsymbol{J}({}^i\boldsymbol{x})$ and the induced source vector $\boldsymbol{y}({}^i\boldsymbol{x})$, which forms the error function $\boldsymbol{f}({}^i\boldsymbol{x})$, can be obtained partially from the linear part of the circuit matrix $\boldsymbol{M}$ and partially from the variable vector ${}^i\boldsymbol{x}$ using nonlinear circuit analysis techniques either in the frequency domain (power series analysis) or in the hybrid domain with Fourier transform techniques (harmonic balance method).

B. Circuit and Jacobian Matrices

The circuit matrix $\boldsymbol{M}(\boldsymbol{x})$ in (2) can be viewed as a matrix composed of K by K block matrices:

$$\boldsymbol{M}(\boldsymbol{x}) = \begin{bmatrix} \boldsymbol{M}_{0,0}(\boldsymbol{x}) & \boldsymbol{M}_{0,1}(\boldsymbol{x}) & \cdots & \boldsymbol{M}_{0,K-1}(\boldsymbol{x}) \\ \boldsymbol{M}_{1,0}(\boldsymbol{x}) & \boldsymbol{M}_{1,1}(\boldsymbol{x}) & \cdots & \boldsymbol{M}_{1,K-1}(\boldsymbol{x}) \\ \vdots & \vdots & \cdots & \vdots \\ \boldsymbol{M}_{K-1,0}(\boldsymbol{x}) & \boldsymbol{M}_{K-1,1}(\boldsymbol{x}) & \cdots & \boldsymbol{M}_{K-1,K-1}(\boldsymbol{x}) \end{bmatrix}. \tag{6}$$

Each block matrix $\boldsymbol{M}_{q,k}(\boldsymbol{x})$ is a matrix with input frequency index k and output, or objective, frequency index q, and has the same $m \times m$ where m is the dimension of the corresponding vector $\boldsymbol{x}_{\omega q}$ in (3). Reducing $\boldsymbol{x}_{\omega q}$ to its minimum required size will always reduce the size of the matrix $\boldsymbol{M}(\boldsymbol{x})$ and decrease the complexity in circuit analysis. The minimum required variables of $\boldsymbol{x}_{\omega q}$ include all the node voltages of the admittance-type nonlinear elements, all the edge currents of the impedance-type nonlinear elements in the circuit, and any node voltages or edge currents of interest for the final results.

Entries in each matrix $\boldsymbol{M}_{q,k}(\boldsymbol{x})$ may not be $\boldsymbol{x}$-dependent because they are generated from all the elements of the circuit. In most cases, linear elements of the circuit create entries in $\boldsymbol{M}_{q,k}(\boldsymbol{x})$ which are independent of the variable $\boldsymbol{x}$, and nonlinear elements add $\boldsymbol{x}$-dependent values to some of the entries. However, by using the modified nodal admittance matrix, some nonlinear elements, such as nonlinear inductors, will create $\boldsymbol{x}$-independent entries as well. If $\boldsymbol{M}_{ID(q,k)}$ represents the modified nodal admittance matrix generated from all the linear elements of the circuit plus those $\boldsymbol{x}$-independent entries generated from all the nonlinear elements of the circuit, we have

$$\boldsymbol{M}_{q,k}(\boldsymbol{x}) = \boldsymbol{M}_{ID(q,k)} + \boldsymbol{M}_{D(q,k)}(\boldsymbol{x})$$

where the $\boldsymbol{x}$-dependent matrix $\boldsymbol{M}_{D(q,k)}(\boldsymbol{x})$ derives from the nonlinear elements, and matrix $\boldsymbol{M}_{ID(q,k)}$ is always a zero matrix if q is not equal to k.

Similarly, the Jacobian matrix $\boldsymbol{J}({}^i\boldsymbol{x})$ in (5) has the same structure as $\boldsymbol{M}(\boldsymbol{x})$ in (6). Each block matrix $\boldsymbol{J}_{q,k}({}^i\boldsymbol{x})$ represents the block Jacobian matrix for input frequency ω_k and objective frequency ω_q and has the same size as

$\boldsymbol{M}_{q,k}(\boldsymbol{x})$. As before, each block Jacobian matrix $\boldsymbol{J}_{q,k}({}^{i}\boldsymbol{x})$ is a combination of two matrices:

$$\boldsymbol{J}_{q,k}({}^{i}\boldsymbol{x}) = \boldsymbol{J}_{ID(q,k)} + \boldsymbol{J}_{D(q,k)}({}^{i}\boldsymbol{x}). \tag{7}$$

The matrix $\boldsymbol{J}_{ID(q,k)}$ in (7) is $\boldsymbol{x}$-independent, and

$$\boldsymbol{J}_{ID(q,k)} = \boldsymbol{M}_{ID(q,k)}.$$

For efficient calculations, each complex independent variable X_j of $\boldsymbol{x}_{\omega q}$ can be separated into real and imaginary parts, and each complex entry $Y_{j,l}$ in matrix $\boldsymbol{J}_{ID(q,k)}$ can also be represented by a 2×2 matrix of real entries:

$$Y_{j,l} = \begin{bmatrix} \mathrm{Re}\{Y_{j,l}\} & -\mathrm{Im}\{Y_{j,l}\} \\ \mathrm{Im}\{Y_{j,l}\} & \mathrm{Re}\{Y_{j,l}\} \end{bmatrix}. \tag{8}$$

Since $\boldsymbol{J}_{ID(q,k)}$ is iteration number i independent, it can be calculated just once. However, the $\boldsymbol{x}$-dependent Jacobian matrix $\boldsymbol{J}_{D(q,k)}({}^{i}\boldsymbol{x})$ can only be obtained using nonlinear analysis and must be reevaluated if a new Newton iteration is required.

In addition to the Jacobian matrix $\boldsymbol{J}({}^{i}\boldsymbol{x})$, solution of the circuit equations (2) using the iterative procedures (5) also requires calculation of the induced source vector $\boldsymbol{y}({}^{i}\boldsymbol{x})$ for each iteration i. Assuming that $\boldsymbol{y}_{\omega q}({}^{i}\boldsymbol{x})$ is the component vector of $\boldsymbol{y}({}^{i}\boldsymbol{x})$ at radian frequency ω_q, the calculation of $\boldsymbol{y}_{\omega q}({}^{i}\boldsymbol{x})$ can be performed as

$$\boldsymbol{y}_{\omega q}({}^{i}\boldsymbol{x}) = \boldsymbol{M}_{ID(q,k)}{}^{i}\boldsymbol{x}_{\omega q} + \boldsymbol{y}_{NL(\omega q)}({}^{i}\boldsymbol{x}), \qquad k = q \tag{9}$$

where $\boldsymbol{y}_{NL(\omega q)}({}^{i}\boldsymbol{x})$ represents the induced source vector of all the nonlinear elements at radian frequency ω_q. Both $\boldsymbol{J}_{D(q,k)}({}^{i}\boldsymbol{x})$ in (7) and $\boldsymbol{y}_{NL(\omega q)}({}^{i}\boldsymbol{x})$ in (9) can be obtained using nonlinear analysis techniques.

C. Block Newton Iteration

Equation (5) is frequently used in nonlinear circuit analysis to minimize the objective function because of its asymptotic rate of convergence. However, evaluation of the whole Jacobian can be time consuming. In a nonlinear circuit the major coupling between currents and voltages is when the components are at the same frequencies. Consequently a modified form of Newton's method [24] (block Newton) can be used.

If the number of frequencies considered in the circuit analyzed is K and the size of each $\boldsymbol{J}_{q,k}({}^{i}\boldsymbol{x})$ is $m\times m$, the dimension of the full Jacobian matrix $\boldsymbol{J}({}^{i}\boldsymbol{x})$ is $mK\times mK$. For a complete Newton's method, $\boldsymbol{J}^{-1}({}^{i}\boldsymbol{x})\boldsymbol{f}({}^{i}\boldsymbol{x})$ must be calculated. For either type of matrix factorization, PLU or QR, the arithmetic cost of the calculation on matrix $\boldsymbol{J}({}^{i}\boldsymbol{x})$ is always proportional to $(mK)^3$. However, from (7), the $\boldsymbol{x}$-independent matrix $J_{ID(q,k)}$ is a nonzero matrix only if $q = k$. For most microwave nonlinear analog circuits, the values of those derivatives in the diagonal blocks $\boldsymbol{J}_{D(q,q)}({}^{i}\boldsymbol{x})$ are normally larger than those values in the off-diagonal blocks $\boldsymbol{J}_{D(q,k)}({}^{i}\boldsymbol{x})$, $q \neq k$. Therefore, by calculating only the diagonal blocks of the Jacobian matrices $\boldsymbol{J}_{q,q}({}^{i}\boldsymbol{x})$ $(q = 0,1,\cdots,K-1)$, the cost of matrix calculation will be K^2 times lower than the cost for calculation of the full Jacobian form. That is, to solve K separate iterative procedures simultaneously,

$${}^{i+1}\boldsymbol{x}_{\omega q} = {}^{i}\boldsymbol{x}_{\omega q} - \boldsymbol{J}_{q,q}^{-1}({}^{i}\boldsymbol{x})\,\boldsymbol{f}_{\omega q}({}^{i}\boldsymbol{x}) \tag{10}$$

where $q = 0,1,\cdots,K-1$. This method uses only the diagonal blocks of the full Jacobian matrix.

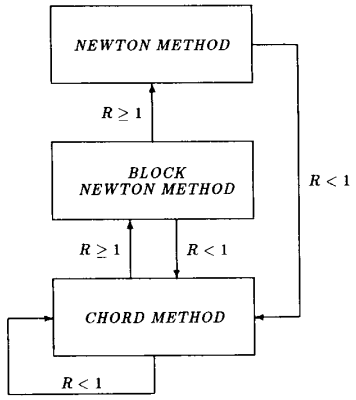

Fig. 1. The algorithm used to determine the method to be used in finding the present iterate value of $\boldsymbol{x}$. R is the ratio between the current converged error and the previous converged error.

Both the Newton and the block Newton method can be combined with the chord method to obtain further computational improvement. The chord method uses the previous $\boldsymbol{J}$ for the present iterative process, regardless of the method used in the previous iteration. This can save considerable Jacobian matrix calculation time and eliminates the need for matrix inversion. The convergence algorithm just described is summarized in Fig. 1.

III. GPSA Arithmetic Operator Method

The GPSA arithmetic operator method (GPSA-AOM) is based on direct complex multiplications and additions. It is similar to the approach taken by Haywood and Chow [25]. However, instead of using the spectrum convolutions, a simple spectrum mapping function is used for each spectral multiplication.

If we consider the system output $y(t)$ to be a function of two independent variables $x(t)$ and $z(t)$,

$$x(t) = \sum_{n=0}^{N} x_n(t) = \sum_{n=0}^{N} |X_n|\cos(\omega_n t + \phi_n)$$

and

$$z(t) = \sum_{m=0}^{M} z_m(t) = \sum_{m=0}^{M} |Z_m|\cos(\omega_m t + \theta_m)$$

the generalized power series for the output $Y_{\omega q}$ at the objective radian frequency ω_q is expressed as

$$Y_{\omega q} = \sum_{\sigma=0}^{\infty}\sum_{\rho=0}^{\infty} a_{\omega q,\sigma,\rho}\left\{\left[\sum_{n=0}^{N} x_n(t-\tau_n)\right]^{\sigma} \cdot\left[\sum_{m=0}^{M} z_m(t-\lambda_m)\right]^{\rho}\right\}_{\omega q} \tag{11}$$

where ω_q is the objective frequency, σ and ρ are the orders of the power series terms, $a_{\omega q,\sigma,\rho}$ are complex coefficients in the frequency domain, and τ_n and λ_m are time delays that depend on the indexes of the input frequency components. The spectrum of x can be represented as a vector:

$$\boldsymbol{s}_x = \frac{1}{2}\left[X_{-\omega K} \quad \cdots \quad X_{-\omega 1} \quad 2X_0 \quad X_{\omega 1} \quad \cdots \quad X_{\omega K} \right]^T \tag{12}$$

where $X_{\omega k} = X^*_{-\omega k}$ and "$*$" indicates the complex conjugate. The spectrum vector for $z(t)$ is similarly defined. For analysis purposes, we may simplify (11) to be an ordinary two-variable-dependent power series by using phase shifting of the spectra of $x(t)$, $z(t)$, and $y(t)$ to eliminate time delays and complex coefficients:

$$y(t) = \sum_{\sigma=0}^{\infty} \sum_{\rho=0}^{\infty} a_{\sigma,\rho} x^{\sigma}(t) z^{\rho}(t). \tag{13}$$

The output spectrum $\boldsymbol{s}_y$ for the basic operation $y = xz$ can be found from the product of $\boldsymbol{s}_x$ and $\boldsymbol{s}_z^T$. Let $\boldsymbol{S}_y$ be the matrix of the product of $\boldsymbol{s}_x$ and $\boldsymbol{s}_z^T$:

$$\boldsymbol{S}_y = \boldsymbol{s}_x \boldsymbol{s}_z^T. \tag{14}$$

Then each element of $\boldsymbol{S}_y$ represents a component of the spectrum of the signal y, and has the value $X_{\omega i} Z_{\omega j}$ and frequency $\omega_i + \omega_j$. By combining the same frequency entries, $\boldsymbol{S}_y$ can be converted into a vector form $\boldsymbol{s}_y$:

$$\boldsymbol{s}_y = \frac{1}{2}\left[Y_{-2\omega K} \quad \cdots \quad 2Y_0 \quad \cdots \quad Y_{2\omega K} \right]^T. \tag{15}$$

The contributions of higher order cross products of $\boldsymbol{s}_x$ and $\boldsymbol{s}_z$ can be obtained using the recursive application of (14) and (15).

Implementation in the Newton iteration process requires derivatives of the value in each entry of vector $\boldsymbol{s}_y$ with respect to all the different independent variables X and Z. These derivatives of each entry in $\boldsymbol{s}_y$ can be obtained by using the chain rule and complex multiplications and additions.

The calculations for system outputs presented in (14) and its derivatives are basic components of GPSA-AOM. Some techniques can also be used to modify this method to obtain increased computational efficiency.

A. Spectrum Limiting

Equation (14) shows that the spectrum vector $\boldsymbol{s}_y$ of the dependent variable $y(t)$ for $y(t) = x(t)z(t)$ can be created from the product of the two spectrum vectors $\boldsymbol{s}_x$ and $\boldsymbol{s}_z$ of the two independent variables $x(t)$ and $z(t)$. However, not all of the entries in $\boldsymbol{s}_y$ are required as objective frequencies, and some of the rest are useful for the higher order calculations only. Calculating those undesired entries will consume much computer computation time and contribute little to the final results. Therefore, if the number of objective frequencies considered in a system is large enough to describe the system nonlinearities, the frequency components of the spectrum of y can be limited to contain these frequencies only. Any additional frequencies which are created by the product of $\boldsymbol{s}_x$ and $\boldsymbol{s}_z$ can be eliminated from $\boldsymbol{s}_y$.

$X_{\omega i}$		$Z_{\omega j}$	
i	k_i	j	k_j
0	+1	1	+1
1	+1	0	+1
2	−1	3	+1
3	+1	2	−1
4	−1	5	+1
5	+1	4	−1
5	−1	6	+1
6	+1	5	−1

(a)

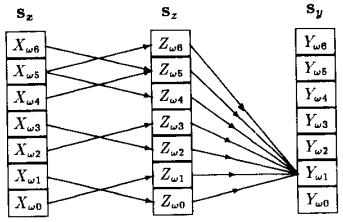

(b)

Fig. 2. An example of *spectrum mapping* for GPSA-AOM. (a) A mapping function used for the objective frequency ω_1. (b) The required complex multiplications for the objective frequency ω_1 using the mapping defined in (a).

B. Spectrum Mapping

To evaluate the nonlinear system output $y(t) = x(t)z(t)$ with *spectrum limiting* on all the dependent and independent variables, some complex multiplications are discarded. These redundant multiplications will also consume much time in frequency searching operations. To avoid this redundancy, a mapping function can be used. This results in considerable computation time reduction when the frequencies under evaluation are poorly correlated.

The spectrum mapping function relates the components of the output spectrum to the spectra of two inputs where the output is the product of the two inputs. Fig. 2 is an example. Assume two sinusoidal signals of 3 GHz and 3.05 GHz are applied to a nonlinear system, and the considered frequencies include all the first- and second-order intermodulation products. For second-order intermodulation product IF(f_1) = 50 MHz, assuming RF(f_2) = 3 GHz and LO(f_3) = 3.05 GHz, the mapping function of $y = xz$ can be set as shown in Fig. 2(a). In Fig. 2(a), i and j represent the frequency indexes used in each multiplication and k being "-1" indicates that the indicated component of X or Z is to be complex conjugated. For instance, if $i = 3$, $k_i = +1$, $j = 2$, $k_j = -1$, the complex multiplication for this combination is $X_{\omega 3} Z^*_{\omega 2}$. Since all the dependent and independent variables are spectrum limited to the same length, the same spectrum mapping function can be used for the product of any two different variables if the considered objective frequency is the same. Moreover, the same function can be used in derivative calculations. Fig. 2(b) illustrates the usage of spectrum mapping to insert all the results of the required complex multiplications of $X_{\omega i}$ and $Z_{\omega j}$ yielding the entry $Y_{\omega 1}$.

C. Power Series Factoring

Factoring of the power series can be used to reduce the amount of computation. Consider a one-dimensional nonlinearity defined by

$$y = a_0 + a_1 x + a_2 x^2 + \cdots + a_N x^N. \tag{16}$$

This requires $(N-1)$ spectral multiplication *operations*.

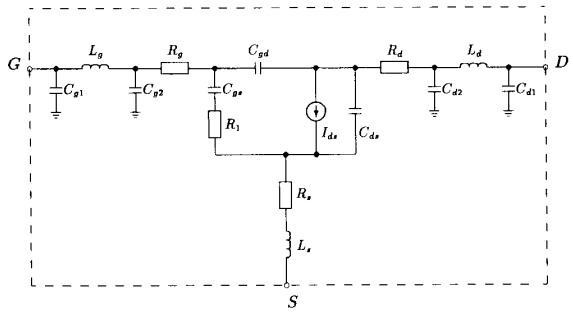

Fig. 3. Circuit used to model the MESFET which includes linear as well as nonlinear elements. Nonlinear elements include C_{gs}, C_{ds}, C_{gd}, and I_{ds}, where I_{ds} is a function of both intrinsic voltages V_{gs} and V_{ds}.

Factoring the power series, the maximum order of x in (16) can be reduced to half,

$$y = \left(b_0 + b_1 x + \cdots + b_{N/2} x^{N/2}\right)^2 + \left(c_0 + c_1 x + \cdots + c_{(N/2)-1} x^{(N/2)-1}\right) \quad (17)$$

if N is even, or

$$y = a_0 + x\left[\left(d_0 + d_1 x + \cdots + d_{(N-1)/2} x^{(N-1)/2}\right)^2 + \left(e_0 + e_1 x + \cdots + e_{(N-3)/2} x^{(N-3)/2}\right)\right] \quad (18)$$

if n is odd. Now $N/2$ (or $(N+1)/2$) *operations* are needed for (17) (or (18)). Each *operation* involves many floating point calculations, and the amount of computation required to factor the power series is relatively small. If N is large, factoring the power series once can result in up to 50 percent reduction in computer time.

IV. Device Characterization

The arithmetic operator method was compared to measurements using a medium-power GaAs MESFET, Avantek AT8250, and the transistor model of Fig. 3. In the equivalent circuit, C_{gs}, C_{gd}, and C_{ds} were taken to be one-dimensional nonlinear elements. The procedure used to determine the model parameters is described in [19], and yielded the linear element values of Table I. With the linear element values fixed, the model of Fig. 3 was optimized to match the measured s parameters at each bias setting, resulting in nonlinear element values as a function of bias voltage. A least-squares technique was used to fit power series to these data. The power series descriptions of the capacitances (C_{gs}, C_{gd}, and C_{ds}) are shown in Table II and their optimized values are compared to their power series representations in Figs. 4 and 5.

The nonlinear element I_{ds} is a function of both intrinsic V_{gs} and V_{ds} (i.e., the voltages across C_{gs} and C_{ds} respectively) and has a bivariate power series description as shown in Table III. Fig. 6 shows the optimized values of the transconductance G_m compared to the values calculated from the bivariate power series expansion. Fig. 7 shows the values of I_{ds} with respect to intrinsic V_{gs} and V_{ds} calculated from this power series. The valid range of this power series description is from $V_{gs} = -1.7$ V to $V_{gs} = 0.75$ V and $V_{ds} = 0.4$ V to $V_{ds} = 5$ V, corresponding to an input power of about 10 dBm.

TABLE I
The Linear Element Values Used in the Model of the Avantek AT-8250 GaAs MESFET

Element	Value
C_{g1}	0.1386 pF
L_g	0.69414 nH
C_{g2}	0.30707 pF
R_g	2.9 Ω
R_s	2.4 Ω
L_s	0.00323 nH
R_d	5.3 Ω
L_d	0.41143 nH
C_{d2}	0.09012 pF
C_{d1}	0.00341 pF
R_1	10 Ω
τ	6.56 pS

TABLE II
The Power Series Coefficients Used in the Model of the Avantek AT-8250 GaAs MESFET

Power Series Coefficients for Nonlinear Elements			
	Element		
Order	C_{ds} (pF)	C_{gs} (pF)	C_{gd} (pF)
0	0.286	0.62039	0.34697
1	−0.022345	0.792475	−0.33135
2	0.0043288	−0.02648	0.1576
3	−0.0003038	−0.22036	−0.032687
4			0.0024389

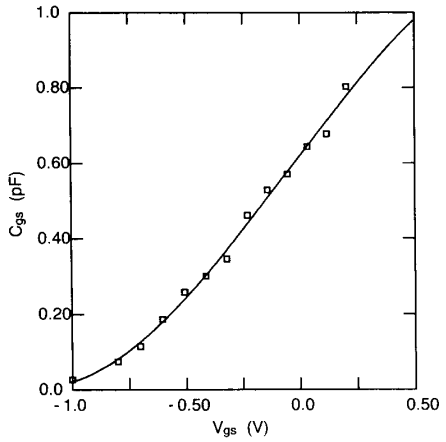

Fig. 4. Optimized values of the gate–source capacitance C_{gs} as a function of gate–source voltage. The points are the optimized values and the curves are the power series representations.

V. Results and Discussion

GPSA-AOM has been implemented in a C language program called FREDA2 (for FREquency Domain Analysis). This is a net-list-based program and can handle arbitrarily large nonlinear analog circuits. Results of simula-

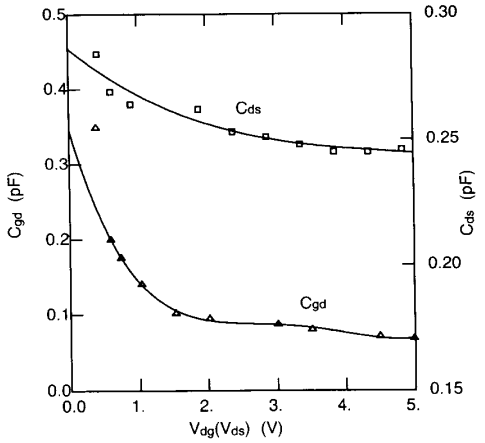

Fig. 5. Optimized values of the drain-source capacitance C_{ds} as a function of drain-source voltage and the gate-drain capacitance C_{gd} as a function of drain-gate voltage. The points are the optimized values and the curves are the power series representations.

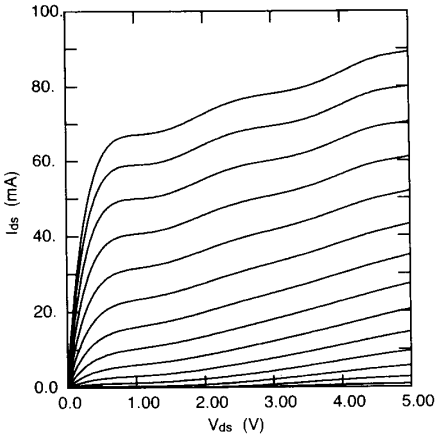

Fig. 7. The drain-source current as a function of intrinsic drain-source voltage for the Avantek AT-8250 GaAs MESFET. The values are calculated from the bivariate power series expression for intrinsic gate-source voltages of −0.8 V to 0.5 V in 0.1 V steps.

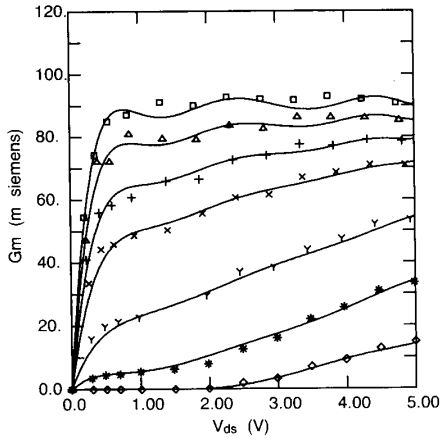

Fig. 6. The transconductance as a function of intrinsic drain-source voltage. Optimized values (points) are compared to the values calculated from the bivariate power series expression for intrinsic gate-source voltages of −0.8, −0.6, −0.4, −0.2, −0.1, 0.0 and 0.1 V.

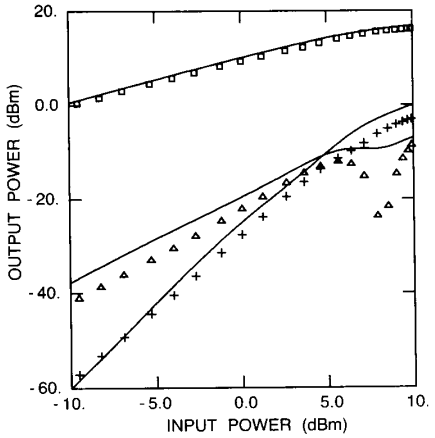

Fig. 8. The results of the single-tone test for the Avantek AT-8250 using a 3 GHz fundamental. Shown are the simulated (curves) and measured values (points) for the power output at the fundamental, the second harmonic, and the third harmonic as a function of input power.

tions using FREDA2 and the two-dimensional circuit model of Fig. 3 are compared to measurements in Figs. 8 and 9 for single-tone and two-tone excitations. The simulated results (curves) are in good agreement with the experimental results (points). Computer run time for the single-tone test is presented in Table IV for various numbers of frequencies considered. Times are given for different input powers (−10, 0, and 10 dBm) with zero initial guess, and for a sweep of the input power from −10 dBm to +10 dBm with 0.5 dB step size. (While sweeping the input power, the initial guesses of the variable values in each power step are based on the final values of the previous step.)

The primary advantage of the arithmetic operator method in frequency-domain spectral balance, compared to the earlier reported table method, is the 2-D model simulation capability. Even with this extended capability, AOM is about ten times faster than TM [19], [26]. AOM has good convergence properties and simulation can be achieved with large input powers and zero initial guess. However, if a sweep of the input power is required, it is more efficient to use the results of the previous lower input power simulation as an initial guess of the circuit variables. We attribute the good convergence properties to the use of analytic derivatives rather than numerical derivatives. The analytic derivatives need to be calculated to double precision to obtain convergence at the higher input power levels if the system nonlinearities are modeled with high-order power series. This level of precision cannot readily be obtained by taking derivatives numerically.

As mentioned in Section II, a mix of the Newton, block Newton, and chord methods is used in the simulation to obtain an efficient simulator. This iteration scheme greatly enhances the speed of FREDA2. For almost every case in the single-tone and two-tone test, one or two block Newton methods followed by several chord methods are enough

TABLE III
THE BIVARIATE POWER SERIES COEFFICIENTS USED FOR I_{ds} IN THE MODEL OF THE AVANTEK AT-8250 GAAS MESFET

Order of V_{gs} Term	Order of V_{ds} Term							
	0	1	2	3	4	5	6	7
0	−0.00001156555	0.07625879	−0.1056094	0.07761516	−0.0313192	0.007058957	−0.0008327161	0.00004002119
1	−0.00006103041	0.3069145	−0.4733609	0.3675621	−0.1555473	0.03641407	−0.00442661	0.0002179638
2	0.002515452	0.3475555	−0.6445519	0.5434066	−0.2414711	0.05823406	−0.007202639	0.0003578266
3	0.01210829	−0.2693955	0.4357904	−0.3522143	0.1566408	−0.03871469	0.004976994	−0.0002589956
4	0.01565735	−0.8516739	1.804808	−1.620442	0.7466659	−0.184505	0.0232377	−0.001171287
5	−0.004989491	−0.2561477	0.7083704	−0.6889429	0.3238367	−0.07946468	0.009787713	−0.0004777891
6	−0.02538143	0.6769809	−1.477119	1.344364	−0.6245825	0.1552918	−0.01966353	0.0009961386
7	−0.01847188	0.6183949	−1.461959	1.367254	−0.6390305	0.1582496	−0.01984881	0.0009928612
8	−0.004226292	0.1523607	−0.3733957	0.3534024	−0.1655718	0.04091728	−0.005108844	0.0002540126

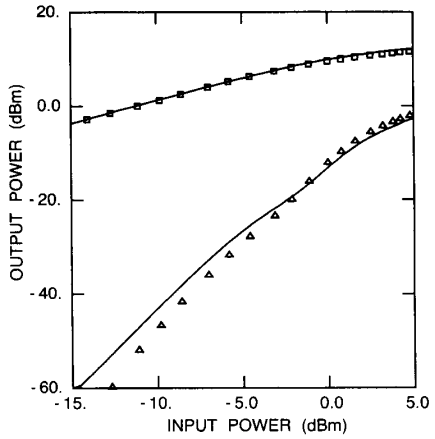

Fig. 9. The results of the two-tone test for the Avantek AT-8250 using two equal-amplitude signals input at 2.35 GHz and 2.4 GHz. Shown are the simulated (curves) and measured values (points) as a function of input power for the power output at 2.35 GHz, and the third-order intermodulation product at 2.3 GHz.

TABLE IV
COMPUTER RUN TIMES FOR THE SINGLE-TONE TEST

No. of Freq.	Input Power −10 dBm	Input Power 0 dBm	Input Power +10 dBm	Input power sweeps from −10 dBm to 10 dBm with step size 0.5 dB
3	1.6	1.9	4	30
4	2.3	2.7	6	53
5	3.1	3.9	8	83
6	4.2	5.1	11	123
7	5.2	6.6	14	173
8	6.7	8.3	17	234
9	8.2	10.3	21	300

Times are given in seconds and were measured on a VAX station 3200. The number of frequencies considered is the number of harmonics plus 1 for dc.

to reduce the system errors to the required limit. Using the Newton method with full Jacobian matrix evaluation instead of the block Newton method will lengthen simulation time by a factor of K^2, where K is the number of objective frequencies.

VI. CONCLUSION

In this paper we presented a new frequency-domain spectral balance method, called generalized power series analysis using the arithmetic operator method (GPSA-AOM). Coupled with an enhanced convergence algorithm using a mix of Newton, block Newton, and chord methods, GPSA-AOM is suited to the analysis of nonlinear analog circuits. The technique is straightforward and can handle two-dimensional nonlinear elements in the frequency domain. The simulation of a MESFET amplifier with single-tone and two-tone inputs was compared to measurements to verify the method.

REFERENCES

[1] N. Wiener, "Response of a nonlinear device to noise," M.I.T. Radiation Lab. Rep. V-16S, Apr. 1942.
[2] E. Bedrosian and S. O. Rice, "The output properties of Volterra systems (nonlinear systems with memory) driven by harmonic and Gaussian inputs," *Proc. IEEE*, vol. 59, pp. 1688–1707, Dec. 1971.
[3] J. J. Bussgang, L. Ehrman, and J. W. Graham, "Analysis of nonlinear systems with multiple inputs," *Proc. IEEE*, vol. 62, pp. 1088–1119, Aug. 1974.
[4] S. Narayanan, "Transistor distortion analysis using Volterra series representation," *Bell Syst. Tech. J.*, vol. 46, pp. 991–1024, May–June 1967.
[5] C. L. Law and C. S. Aitchison, "Prediction of wide-band power performance of MESFET distributed amplifiers using the Volterra series representation," *IEEE Trans. Microwave Theory Tech.*, vol. MTT-34, pp. 1308–1317, Dec. 1986.
[6] R. A. Minasian, "Intermodulation distortion analysis of MESFET amplifiers using Volterra series representation," *IEEE Trans. Microwave Theory Tech.*, vol. MTT-28, Jan. 1980.
[7] M. Fliess, M. Lamnabhi, and F. Lamnabhi-Lagarrigue, "An algebraic approach to nonlinear functional expansions," *IEEE Trans. Circuits Syst.*, vol. CAS-30, pp. 554–570, Aug. 1983.
[8] M. Lamnabhi, "A new symbolic calculus for the response of nonlinear systems," *Syst. and Control Lett.*, vol. 2, pp. 154–162, Oct. 1982.
[9] M. Lamnabhi, "Functional analysis of nonlinear circuits: A generating power series approach," *Proc. Inst. Elec. Eng.*, vol. 133, Pt. H, pp. 375–384, Oct. 1986.
[10] C. A. A. Wass, "A table of intermodulation products," *J. Inst. Elec. Eng.*, vol. 95, Part III, pp. 31–39, 1948.
[11] G. M. Engel, D. A. Conner, and W. J. Steen, "Determination of intermodulation product amplitudes," in *Proc. 1967 Nat. Electron. Conf.*, pp. 719–723.
[12] R. G. Sea, "An algebraic formula for amplitudes of intermodulation products involving an arbitrary number of frequencies," *Proc. IEEE*, vol. 56, pp. 1388–1389, Aug. 1968.
[13] R. G. Sea and A. G. Vacroux, "On the computation of intermodulation products for a power series nonlinearity," *Proc. IEEE*, pp. 337–338, Mar. 1969.
[14] G. L. Heiter, "Characterization of nonlinearities in microwave devices and systems," *IEEE Trans. Microwave Theory Tech.*, vol. MTT-21, pp. 797–805, Dec. 1973.
[15] R. S. Tucker and C. Rauscher, "Modelling the 3rd-order intermodulation-distortion properties of a GaAs FET," *J. Electron Lett.*, vol. 13, pp. 508–509, Aug. 1977.
[16] R. S. Tucker, "Third-order intermodulation distortion and gain compression in GaAs FET's," *IEEE Trans. Microwave Theory Tech.*, vol. MTT-27, pp. 400–408, May 1979.

[17] J. A. Higgins and R. L. Kuvas, "Analysis and improvement of intermodulation distortion in GaAs power FET's," *IEEE Trans. Microwave Theory Tech.*, vol. MTT-28, pp. 9–17, Jan. 1980.

[18] M. B. Steer and P. J. Khan, "An algebraic formula for the complex output of a system with multi-frequency excitation," *Proc. IEEE*, pp. 177–179, Jan. 1983.

[19] G. W. Rhyne and M. B. Steer, "Generalized power series analysis of intermodulation distortion in a MESFET amplifier: Simulation and experiment," *IEEE Trans. Microwave Theory Tech.*, vol. MTT-35, pp. 1248–1255, Dec. 1987.

[20] G. W. Rhyne, M. B. Steer, and B. D. Bates, "Frequency-domain nonlinear circuit analysis using generalized power series," *IEEE Trans. Microwave Theory Tech.*, vol. 36, pp. 379–387, Feb. 1988.

[21] G. W. Rhyne, "Computer aided analysis of nonlinear microwave analog circuits," Ph.D. thesis, CCSP-TR-23, North Carolina State University, Raleigh, NC, 1988.

[22] J. E. Dennis and R. B. Schnabel, *Numerical Methods for Nonlinear Equations and Unconstrained Optimization*. Englewood Cliffs, NJ: Prentice-Hall, 1983.

[23] J. Vlach and K. Singhal, *Computer Methods for Circuit Analysis and Design*. New York: Van Nostrand Reinhold, 1983.

[24] J. M. Ortega and W. C. Reinboldt, *Iterative Solution of Nonlinear Equations in Several Variables*. New York: Academic Press, 1970.

[25] J. H. Haywood and Y. L. Chow, "Intermodulation distortion analysis using a frequency-domain harmonic balance technique," *IEEE Trans. Microwave Theory Tech.*, vol. 36, pp. 1251–1257, Aug. 1988.

[26] C. R. Chang *et al.*, "Simulation of nonlinear RF and microwave circuits," in *RF Expo East 1988 Proc.*, Oct. 1988, pp. 333–342.

✠

Chao-Ren Chang received the B.S. degree from National Cheng Kung University, Taiwan, Republic of China, in 1971 and the M.S. degree from North Carolina State University in 1980, both in electrical engineering.

From 1976 to 1979 and from 1981 to 1984, he was an assistant scientist in the Microwave Laboratory of the Chung Shan Institute of Science and Technology, Taiwan. Since 1984 he has been a teaching and research assistant at North Carolina State University, Raleigh, where he is currently completing the Ph.D. degree in electrical engineering. His research interests are in the areas of the computer-aided analysis, design and testing of nonlinear microwave circuits, and the characterization of microwave devices.

✠

Michael B. Steer (S'78–M'82) received the Ph.D. degree in electrical engineering from the University of Queensland, Brisbane, Australia, in 1983.

He is currently Assistant Professor of Electrical and Computer Engineering at North Carolina State University. His research involves the simulation and computer-aided design of nonlinear analog circuits with large-signal excitation and of circuits with mixed analog and digital signals. He is currently working on the simulation of microwave analog circuits, delta–sigma modulators, high-speed printed circuit boards, and the computer-aided design of analog circuits using simulated annealing.

In 1987 Dr. Steer was named a Presidential Young Investigator.

✠

George W. Rhyne (S'81–M'87) received the B.S., M.S., and Ph.D. degrees in electrical engineering from North Carolina State University, Raleigh, in 1982, 1985, and 1988 respectively.

In 1988 he joined the Defense Systems and Electronics Group of Texas Instruments, Dallas, TX, as a microwave design engineer. He is currently involved in device characterization and modeling as well as in the development of circuits and systems for use in airborne phased-array applications.